Available online at www.sciencedirect.com

SCIENCE DIRECT®

Journal of Volcanology and Geothermal Research 146 (2005) 8–25

Journal of volcanology and geothermal research

www.elsevier.com/locate/jvolgeores

The submarine flanks of Anatahan Volcano, commonwealth of the Northern Mariana Islands

William W. Chadwick Jr.[a,*], Robert W. Embley[b], Paul D. Johnson[c], Susan G. Merle[a], Shannon Ristau[b], Andra Bobbitt[a]

[a]*Oregon State University/NOAA, Hatfield Marine Science Center, 2115 SE OSU Drive, Newport, OR 97365-5258, USA*
[b]*NOAA/Pacific Marine Environmental Laboratory, Newport, OR 97365, USA*
[c]*SOEST/HMRG, University of Hawaii, Honolulu, HI 96822, USA*

Received 9 August 2004; accepted 3 November 2004

Abstract

The submarine flanks of Anatahan volcano were surveyed comprehensively for the first time in 2003 and 2004 with multibeam and sidescan sonar systems. A geologic map based on the new bathymetry and backscatter data shows that 67% of the volcano's submarine flanks are covered with volcaniclastic debris and 26% is lava flows, cones, and bedrock outcrops. The island of Anatahan is only 1% of the volume of the entire volcano, which has a height from its submarine base of 3700 m and an average diameter of ~35 km. NE Anatahan is a prominent satellite volcano located 10 km NE of the island, but it is only 6% of Anatahan's volume (40 km^3 vs. 620 km^3). Seventy-eight submarine eruptive vents are mapped associated with lava flows and cones between depths of 350 and 2950 m, and 80% of these vents are located in a cluster on the east flank of the volcano. The distribution of cones and lava flows vs. depth suggests a possible change in eruptive style from explosive to effusive between 1500 and 2000 m. Eruptive vents below 2000 m have produced mostly lava flows. There is no evidence of major landslides on the submarine flanks of Anatahan volcano, in contrast to many basaltic islands and seamounts, suggesting that mass wasting at felsic oceanic arc volcanoes may be characterized by sediment flows of unconsolidated volcaniclastic debris instead of mass movements of relatively large intact blocks.

Keywords: Anatahan volcano; Mariana arc; seafloor mapping; submarine volcano morphology; multibeam and sidescan sonar surveys

1. Introduction

Anatahan is an island volcano located at 16°21′N/145°41′E in the central Mariana volcanic arc of the western Pacific (Fig. 1), whose first historical eruption occurred in May 2003 (Wiens et al., 2004; Trusdell et al., 2005—this issue). The island is 10 km long, 4 km

* Corresponding author. Tel.: +1 541 867 0179; fax: +1 541 867 3907.
E-mail address: bill.chadwick@noaa.gov (W.W. Chadwick).

0377-0273/$ - see front matter © 2005 Elsevier B.V. All rights reserved.
doi:10.1016/j.jvolgeores.2004.11.032

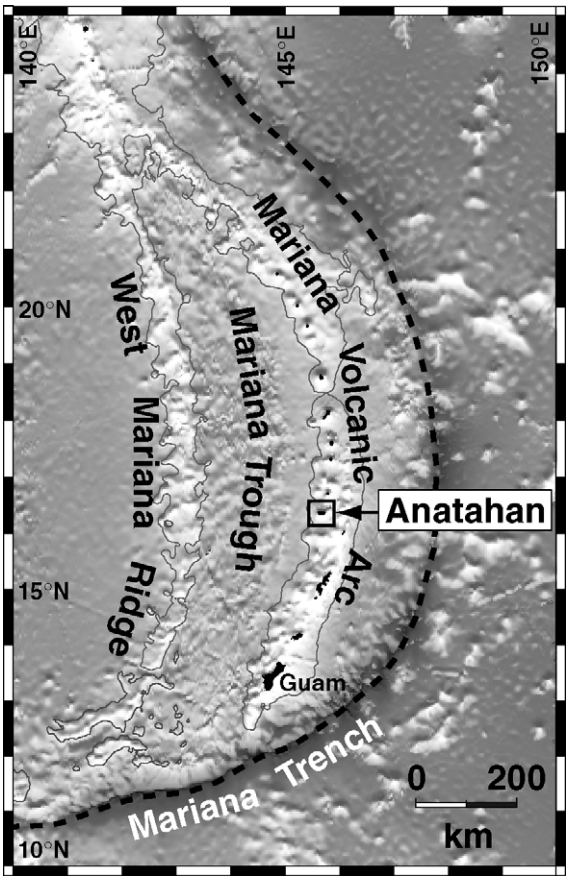

Fig. 1. Location map of Anatahan volcano in the Mariana volcanic arc.

wide, and is elongated in the east–west direction. Anatahan has a maximum elevation of 788 m, but its submarine flanks descend to depths of 2000–3000 m, and therefore most of the volcano lies below sea level. Until recently, little was known about the submarine parts of the volcano except from previous narrow-beam surveys (US Navy SASS data) and one dredge collected nearby (Bloomer et al., 1989; Stern and Hargrove, 2003). In the spring of 2003, the submarine flanks around Anatahan were surveyed with both multibeam and sidescan sonar systems, providing new bathymetry and backscatter imagery of the majority of the volcano that is hidden underwater. This was part of a larger survey of more than 50 submarine volcanoes within the Mariana volcanic arc between 13°10′N and 23°10′N (Embley et al., 2004). Supplementary multibeam data were collected on two other expeditions to the area in the fall of 2003 and the spring of 2004. This was part of the Submarine Ring of Fire project, which is a multi-year study of seafloor volcanism in the western Pacific funded by NOAA's Ocean Exploration and Vents Programs (see: http://oceanexplorer.noaa.gov/ and http://www.pmel.noaa.gov/vents/). The new data from Anatahan provide the first information on the location, extent, and style of submarine volcanism on the flanks of the volcano.

2. Sources of data and methods

In this paper, we present new maps of Anatahan volcano, which include data above and below sealevel compiled from several different sources. A digital elevation model (DEM) of Anatahan island was created by Steve Schilling (U.S. Geological Survey/Cascades Volcano Observatory) by digitizing contours from a topographic map and then georeferencing it with handheld GPS positions provided by Frank Trusdell (U.S. Geological Survey/Hawaiian Volcano Observatory). The DEM has a grid-cell size of 10 m.

Bathymetric data provide information on the morphology and depth of the seafloor as well as the shape and size of submarine features (Fig. 2a). Bathymetry around Anatahan was collected primarily using the EM300 hull-mounted multibeam-sonar system on the *R/V Thomas G. Thompson* during expeditions along the Mariana arc in February 2003 and April 2004. The EM300 system is a 30 kHz echo sounder with 135 beams per ping in the cross-track direction. The swath width and spatial resolution are a function of water depth, but in general the swath is about 3 times as wide as the water depth and in this area we have grided the bathymetry at a 35-m cell size.

Initially, EM300 bathymetry in the Anatahan area was collected during a sidescan-sonar survey of the Mariana arc (described below). The track spacing of the sidescan survey (~9 km) provided full coverage for the sidescan imagery but not for the bathymetry, which has a narrower swath width. Some of the resulting gaps between the north–south tracks in the EM300 bathymetry were filled during transits in 2003 and 2004. Additional bathymetry was collected by the *R/V Onnuri* in September 2003 using a 12 kHz Seabeam2000 multibeam-sonar system (Fig. 2b). The Seabeam2000 data are considerably noisier and lower

in resolution than the EM300 data, and so they are only used where EM300 coverage is lacking in our compilation.

To make a compilation grid of topography and bathymetry (Fig. 2a), the island DEM and the multibeam sonar data were combined and grided together, and any data gaps (such as in the shallow near-shore areas around the island) were filled by interpolation (Fig. 2b). Then the EM300 bathymetry was overlain on the combined grid, so that the highest resolution data are used wherever available. This was done using the MbSystem and GMT software packages (Wessel and Smith, 1991; Caress et al., 1996), and then all the data were brought into ArcGIS for analysis, visualization, and geologic classification. Contour maps, shaded relief maps, and slope maps were made from the compilation grid to aid in interpreting the geology of the volcano.

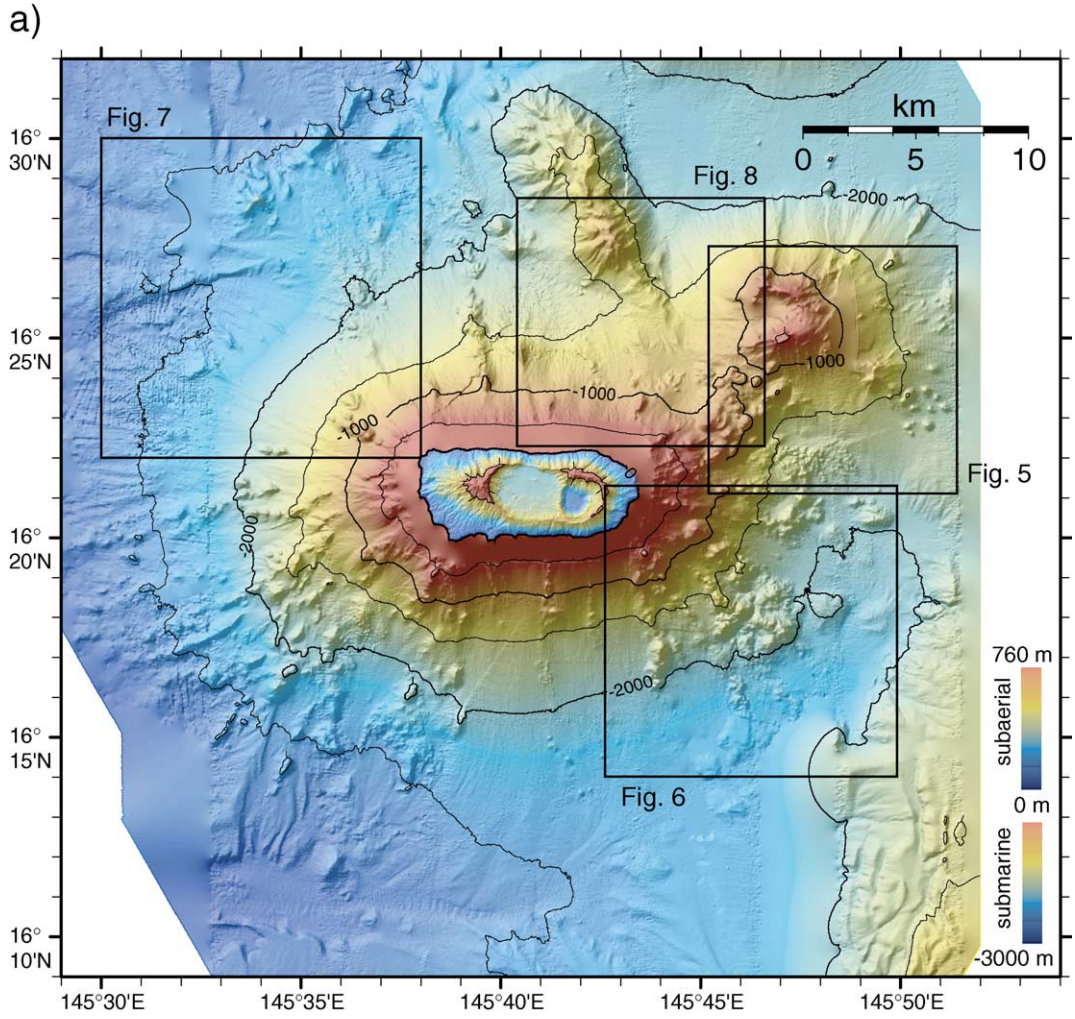

Fig. 2. (a) Map showing grided compilation of topographic and bathymetric data at Anatahan volcano, with 500-m contours and displayed with artificial illumination from the northwest. Note the same range of colors is repeated above and below sealevel. (b) Same map area showing sources of data in the compilation: digital elevation model (DEM) of Anatahan island (horizontal lines), EM300 multibeam sonar bathymetry (stipple), and Seabeam2000 multibeam sonar bathymetry (diagonal lines). The grid is interpolated across data gaps (black). Boxes show the areas of Figs. 5–8. The NE–SW-trending line that crosses the 1000-m contour between the Figs. 7 and 8 boxes is an artifact from the mismatch between EM300 and SeaBeam2000 data.

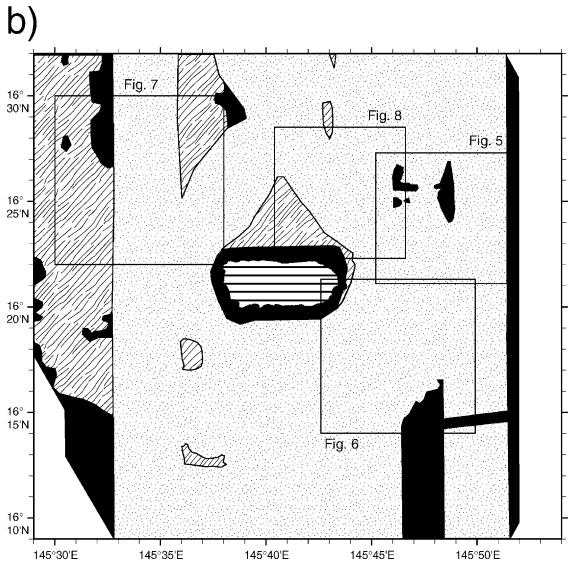

Fig. 2 (*continued*).

Sidescan sonar provides a fundamentally different view of the seafloor that is complimentary to bathymetric data, because it highlights the relative acoustic reflectivity of the bottom rather than its depth (Fig. 3). The MR1 sidescan sonar system, operated by the Hawaii Mapping Research Group at the University of Hawaii, was used to survey a portion of the Mariana arc from 15°40′N to 23°20′N on the *R/V Thomas G. Thompson* in February 2003. The MR1 system uses frequencies of 11 and 12 kHz, and is towed behind the ship at a depth of about 100 m (just below the thermocline) at a survey speed of ~9 knots. Sound is sent outward to either side of the towfish and the strength of the acoustic reflection gives information on the morphology, texture, and structure of the seafloor. For example, lava flows on a sedimented bottom can be mapped by their high acoustic reflectivity compared to their surroundings. High reflectivity can also be caused by steep slopes, rough surface texture, or fault scarps facing toward the sidescan towfish. Low reflectivity can be due to thick sediment, smooth texture, or acoustic shadows behind hills or scarps. In this paper, high acoustic reflectivity is displayed in the sidescan imagery as black and low reflectivity as white, with a continuous gradient in-between (Fig. 3).

The acoustic reflectivity in sidescan imagery is also influenced by the insonification direction relative to seafloor features. For example, a hill might have high reflectivity on the side facing the sidescan towfish, but low reflectivity on the side facing away. The dashed lines in Fig. 3 show the tracklines during the sidescan survey and the open arrows show the insonification direction to either side of these tracks. No information is returned directly under the sidescan towfish tracks. The first acoustic multiple (a bounce from the bottom and ocean surface back to the towfish) can create a linear artifact in the sidescan imagery, especially in areas of low reflectivity (Fig. 3). The spatial resolution of the MR1 sidescan data is a function of water depth and distance outward from the towfish to either side. The acoustic returns are digitized into 1024 pixels on each side of the towfish. The swath width of the MR1 system is about 7.5 times water depth and the data from this survey were grided at a 16-m cell size. We chose to use a track spacing of ~9 km during the survey, and the swath width of ~15 km provided about 40% overlap between adjacent lines in most areas (Fig. 3). The MR1 system can also provide phase difference bathymetry, but since it is lower in resolution than the EM300 data and gives about the same spatial coverage it is not presented in this paper.

3. Submarine geological classification scheme

We divided the submarine flanks of Anatahan into geologic units and mapped structures based on the combined bathymetry and sidescan dataset (Fig. 4). This classification scheme is based on the morphology and backscatter characteristics of submarine features. The categories are somewhat general due to the lack of ground-truth data that would allow more specific classification (near-bottom visual observations or direct sampling). If these kinds of data are collected in the future, then the mapped units could be made more specific. An approximate age progression among the units can be established based on their morphology and acoustic reflectivity. Characteristics that we associate with increasing age include morphologic evidence of erosion or mass wasting, a high fault density, and low acoustic reflectivity where the morphology suggests that it is likely due to significant pelagic sediment accumulation over rocky outcrops. The units interpreted to be the youngest are characterized by high

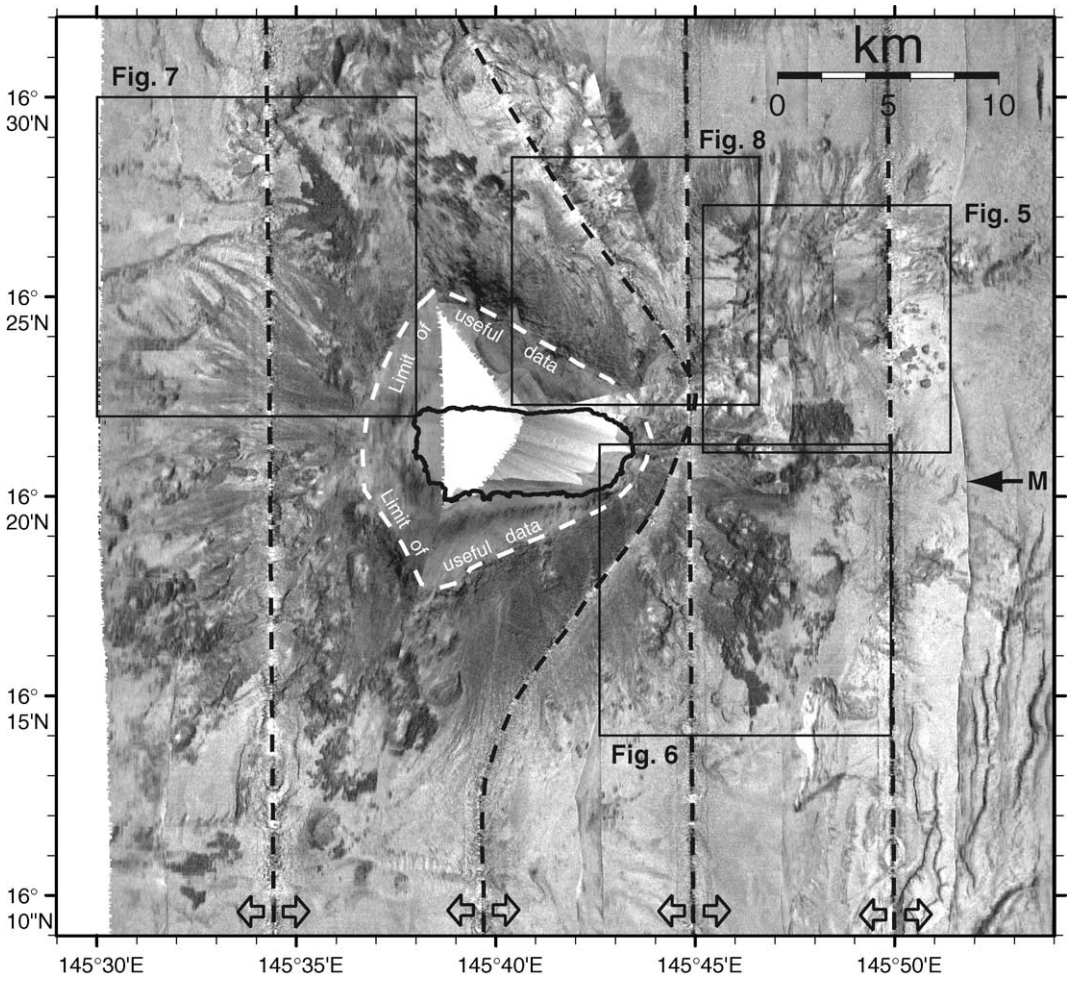

Fig. 3. Sidescan sonar imagery of the submarine flanks of Anatahan volcano (areas of relatively high acoustic reflectivity are dark and areas of low reflectivity are light). Coast of Anatahan island is shown by solid black line. Area of no valid sidescan data around the island is bound by a white dashed outline. Black dashed lines show survey tracklines (and the nadir below the towfish where no data is collected). Open arrows at bottom show insonification direction from the sidescan towfish to either side of the tracklines. Note adjacent sidescan swaths have about 40% overlap and only data that is closest to nadir are displayed. In other words, the boundary between data from adjacent swaths in the figure is midway between the tracklines. The arrow labeled "M" points to a linear artifact from an acoustic multiple (most prominent in areas of low reflectivity). Boxes show the areas of Figs. 5–8.

reflectivity and an uneroded constructional volcanic morphology.

The broadest subdivision in the geologic units is between the volcanic terrain of Anatahan and NE Anatahan and the older surrounding terrain (Fig. 4). In addition, structures such as faults, crater rims, and eruptive vents are mapped. A description of all the geologic units and how they are defined is given below and is summarized in Table 1.

We have subdivided the volcanic terrain that makes up Anatahan and NE Anatahan into the following geologic units (roughly in order of increasing apparent age): *lava flows*, *cones*, *bedrock outcrops*, *landslide blocks*, *volcaniclastic aprons*, and *domes*. *Lava flows* are characterized by distinctive lobate outlines, high acoustic reflectivity, low relief, and a rugged surface texture. *Cones* also have high acoustic reflectivity, but have a conical mor-

phology with high relief and smooth uneroded slopes. *Cones* are often found in hummocky clusters and lava flows extend downslope from some of them. Both the *lava flows* and the *cones* appear to be relatively young because of their high acoustic reflectivity and undegraded morphology. *Bedrock outcrops* are coherent, resistant ridges that are generally linear and oriented in a radial direction from the island, and have medium acoustic reflectivity. Because the *bedrock outcrops* appear to be somewhat eroded they are probably older features than the *cones*. Alternatively, they could be formed by thick pasty lava flows that naturally disintegrate on steep slopes. *Landslide blocks* are relatively large coherent angular blocks that appear to have been transported gravitationally downslope. At other volcanoes, landslide blocks (or "slumps") are distinguished from debris avalanches (Moore et al., 1989; Moore and Chadwick, 1995), but no debris avalanche deposits are recognized on the submarine slopes of Anatahan. The *volcaniclastic aprons* at Anatahan and NE Anatahan are defined as the material that mantles most of the smooth submarine slopes. The outer edge of the *volcaniclastic aprons* is defined by a distinct break in slope in most places. The aprons are low to medium in acoustic reflectivity and are locally channelized. Much of this unit appears to be fragmental volcanic debris and is probably generated by a combination of processes, including large pyroclastic eruptions from the island that deposit material beyond the shoreline (for Anatahan's apron), erosion or disruption of subaerial lava flows at the coast during or after their emplacement (for Anatahan), or submarine pyroclastic/hydroclastic eruptions and the mechanical breakdown of other submarine eruptive products (for both Anatahan and NE Anatahan). Finally, *domes* are defined as conical or dome-like constructional features, that have low to medium acoustic reflectivity and medium relief (in contrast to the high reflectivity and high relief of the *cones*). Most of the *domes* we have mapped are located near the outer edge of the Anatahan volcaniclastic apron.

The older terrain surrounding Anatahan and NE Anatahan includes the following map units: *constructional ridges*, *abyssal sediment*/*abyssal channels*, and *older arc terrain*. *Constructional ridges* are high relief volcanic terrain located beyond the extent of the *volcaniclastic aprons* of Anatahan and NE Anatahan. Therefore, the *constructional ridges* are features that probably pre-date Anatahan and NE Anatahan. *Abyssal sediment* includes smooth, low-relief, low-reflectivity areas beyond the extent of the *volcaniclastic aprons*. *Abyssal channels* are well-defined, low-relief channels that transport sediments into deeper water to the west. Sediment waves, which appear to be large-amplitude, large-wavelength megaripples, have been mapped around some of the other Mariana islands and seamounts (Embley et al., 2003, 2004, unpublished data), but are not found on the submarine flanks of Anatahan. *Older arc terrain* is characterized by high-relief, very low-reflectivity, and extensive normal faulting, which together are evidence of its much greater age. In the Anatahan area this *older arc terrain* is located to the SE of the island, and is identified as frontal arc uplift of late Eocene or early Oligocene age by Stern et al. (2003).

Submarine eruptive vents are mapped as points associated with *lava flows* and *cones* on Anatahan and NE Anatahan. It is assumed that the summit of each clearly constructional *cone* or the upslope end of each *lava flow* overlies an eruptive vent. The only large submarine crater rim is mapped at the summit of NE Anatahan. Normal faults are mapped where scarps are evident in the bathymetry and/or sidescan data. The sense of displacement across the faults can be determined from a combination of depth offsets in the bathymetry and/or acoustic reflectivity in sidescan sonar imagery. A fault facing toward the sidescan towfish reflects sound back, whereas a fault facing away from the towfish creates an acoustic shadow.

The calculated areas of each geologic unit within the map area of Fig. 4 are listed in Table 1. Two-thirds of the map area is covered with *volcaniclastic aprons* or *abyssal sediment*, whereas *lava flows*, *cones*, and *bedrock outcrops* together occupy 12.5% of the area mapped (Table 1).

4. Discussion

In the Anatahan area, there is a regional slope from the shallower older arc terrain in the east to the deeper terrain of the Mariana Trough to the west (Figs. 1 and 2). Anatahan has previously been described as possibly two coalesced volcanoes

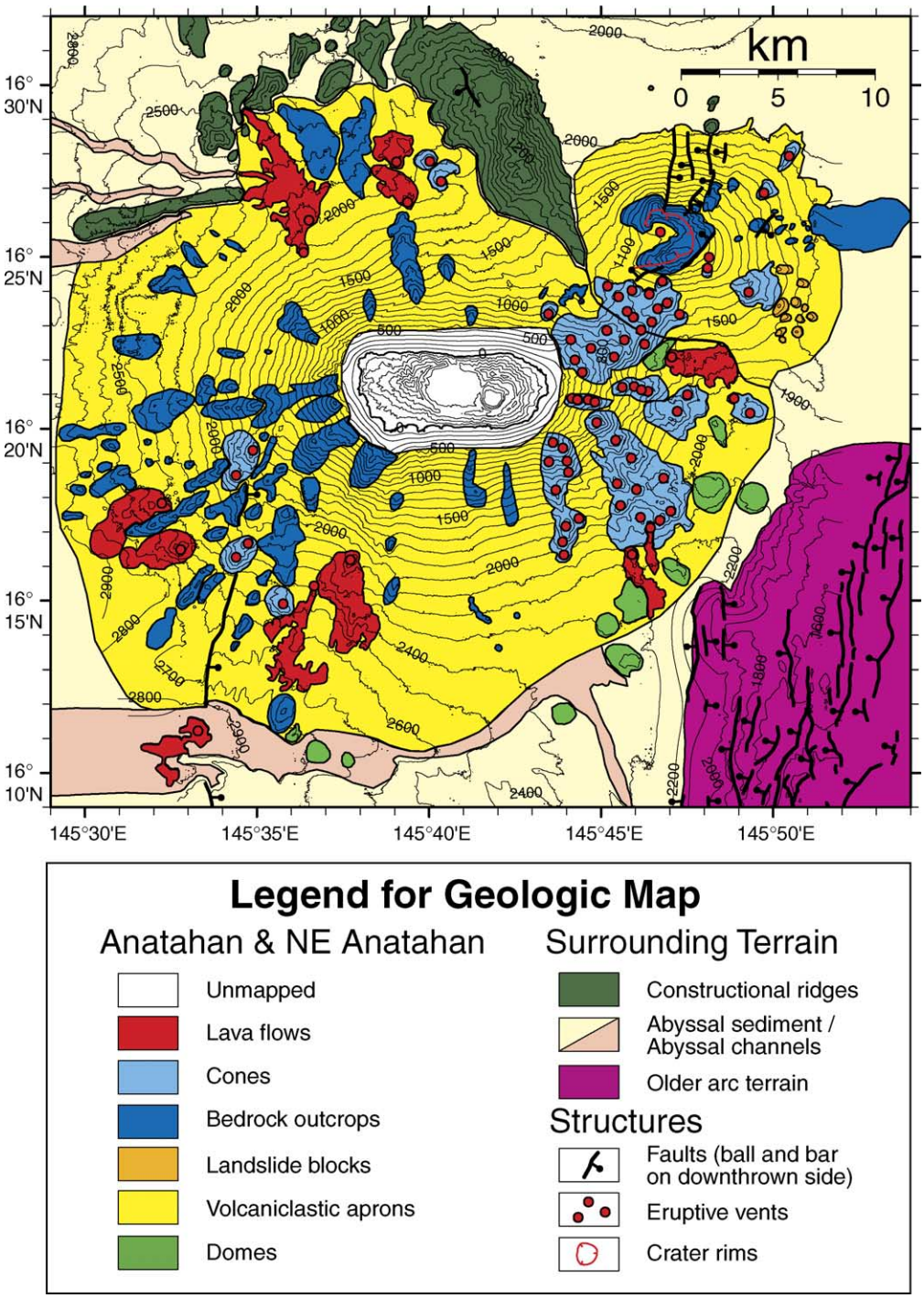

Fig. 4. Geologic map of the submarine flanks of Anatahan volcano, based on the data in Figs. 2 and 3. Legend shows mapped geologic units and structures. A description of the units and their calculated areas is provided in Table 1 and in the text.

Table 1
Descriptions and calculated areas of submarine geologic units around Anatahan

Submarine geologic units	Description	Area ($\times 10^6$ m^2)	Area (% of area mapped)
Anatahan and NE Anatahan			
Unmapped	Areas that lack bathymetry or sidescan coverage, including the island	67	3.1
Lava flows	Lobate outlines, high-reflectivity, low-relief and rugged surface texture	63	2.9[a]
Cones	Conical morphology, high-reflectivity, high-relief, smooth uneroded slopes, often in clusters	88	4.1[a]
Bedrock outcrops	Coherent resistant ridges, medium-reflectivity, appear somewhat eroded, usually oriented radial to the volcano	119	5.5[a]
Landslide blocks	Coherent angular blocks with higher reflectivity than surroundings and appear to have been transported gravitationally downslope	3	0.2
Volcaniclastic aprons	Smooth material that mantles most of the submarine slopes, low to medium reflectivity, locally channelized	698[b]	32
Domes	Dome-like constructional features with low-reflectivity and medium-relief	19	0.9
Surrounding terrain			
Constructional ridges	High-relief constructional features located beyond the extent of the *volcaniclastic aprons* and probably older	88	4.0
Abyssal sediment/Abyssal channels	Smooth, low-relief, low-reflectivity areas beyond the extent of the *volcaniclastic apron*/Well-defined, low-relief channels that transport sediments into deeper water	727/114	34/5.3
Older arc terrain	High-relief, very low-reflectivity, extensively faulted	197	9.1
Structures			
Faults	Normal fault scarps (ball and bar on map symbol are on downthrown side of fault)	n/a	n/a
Eruptive vents/Crater rims	Eruptive vents associated with *lava flows* and *cones*/Rim of summit crater at NE Anatahan	n/a	n/a

[a] The area of *lava flows*, *cones*, and *bedrock outcrops* combined are 12.5% of the total mapped area (the area of Fig. 4 is 2163×10^6 m^3), but amount to 26% of the area within the *volcaniclastic aprons* of Anatahan and NE Anatahan (1038×10^6 m^3).
[b] This value is the area of the Anatahan and NE Anatahan *volcaniclastic aprons* (1038×10^6 m^3) minus the area of the geologic units within their perimeters (340×10^6 m^3).

because of its elongated shape with two peaks and large overlapping calderas at the center of the island (Tanakadate, 1940; Rowland et al., 2005—this issue), but this is not reflected in the bathymetry. Below sealevel, Anatahan appears to be a single volcano (Fig. 2), suggesting that perhaps the east–west elongation is simply due to the existence of aligned eruptive vents with this orientation on the island (Rowland et al., 2005—this issue). Likewise, below sealevel, the majority of the *cones* and *bedrock outcrops* are located on the east and west flanks (Fig. 4). From the base to the summit, Anatahan volcano is 3700 m in height, only a fifth of which is above sealevel. The base of the volcano is roughly circular with an average diameter of ~35 km, compared to the 4×10 km dimensions of the island.

The most prominent feature in the bathymetry around Anatahan is a satellite submarine volcano located about 10 km NE of the island (Figs. 4 and 5), here named NE Anatahan volcano. NE Anatahan volcano has its own *volcaniclastic apron*, which is 13% of the area of the apron of Anatahan. The volume of NE Anatahan is 40 km^3, only 6% of the volume of its larger neighbor (Table 2). NE Anatahan is 10–15 km in diameter at its base, about a half or a third of that of Anatahan. The summit of NE Anatahan volcano reaches a depth of 460 m, and the saddle between NE Anatahan and the submarine flank of Anatahan is at 1030 m. NE Anatahan volcano has a large summit crater with a semi-circular rim that is open to the west (Fig. 5). The floor of the crater is at a depth of 885 m, making the crater walls 425 m high. Most of the summit of NE Anatahan (an area ~5 km in diameter) is mapped as bedrock outcrop, and probably consists of massive lava flows or domes (Figs. 4 and 5). The crater in the middle of the summit is ~2 km across, rivaling

the size of the active eastern crater on the island of Anatahan (Rowland et al., 2005—this issue). The large summit crater on NE Anatahan is evidence of past explosive eruptions from this submarine volcano.

Normal faults are mapped cutting the summit and north flank of NE Anatahan (Figs. 4 and 5). The pattern of faults and their sense of offset suggest that they have accommodated extension centered on the volcano. The strike of the faults changes from NE–SW south of the summit to N–S to the north, perhaps because the regional stress field (E–W extension) interacts with radial stress fields from magma reservoirs beneath Anatahan and NE Anatahan. The orientation of the faults between the volcanoes may be more influenced by the radial volcanic stresses than by the regional tectonic stress field. Only one fault is mapped on the SW slope of Anatahan volcano (Fig. 4). The fact that more faults are mapped on NE Anatahan than on Anatahan suggests that Anatahan is more active, and recent volcanic products probably cover up evidence of previous faulting on Anatahan's submarine flanks.

The only landslide deposits identified in the map area are located southeast of the summit of NE Anatahan volcano (Figs. 4 and 5). Eleven *landslide blocks* are mapped within a 2×4 km area. Each block is between 300–1000 m in diameter and 20–160 m in height, measured from the upslope side (or 2–3 times as high measured from the downslope side). These are identified as *landslide blocks* for the following reasons: (1) we interpret that these features are not eruptive vents, even though they appear conical in the bathymetry, because they appear distinctly angular and blocky in the sidescan imagery (Fig. 5), and (2) these features are not found within a larger area of volcanic constructional morphology with similar acoustic reflectivity, in contrast to the cluster of *cones* mapped SW of the summit of NE Anatahan. Instead these features stand out with different morphology and higher reflectivity than their surroundings (Fig. 5). This suggests that they were transported downslope to their current position rather than formed in place. There is no obvious avalanche debris around the landslide blocks, but the blocks are located downslope from a *cone* and the *bedrock outcrops* making up the summit of NE Anatahan (Fig. 5).

The lack of major landslides around Anatahan is in contrast to the many other oceanic volcanoes where large submarine slumps and debris avalanches have been mapped (Lénat et al., 1989; Moore et al., 1989; Holcomb and Searle, 1991; Borgia et al., 1992), although most of these are basaltic in composition. Our bathymetry and sidescan data show that most of the other submarine volcanoes in the rest of the Mariana arc also lack major landslide deposits (Embley et al., 2003, 2004, unpublished data). Perhaps one reason is that the Mariana volcanoes generally lack well-defined rift zones and a weak underlying sediment layer, which are believed to be responsible for volcano spreading and flank instability in oceanic basaltic volcanoes (Nakamura, 1980; Dieterich, 1988; Borgia, 1994). In addition, the felsic composition and the high proportion of clastic materials erupted by arc volcanoes may lead to fundamentally different modes of mass wasting in the submarine environment. Instead of rare large-volume slumps and avalanches containing varying proportions of intact blocks, arc volcanoes appear to primarily shed unconsolidated volcaniclastic debris. These fluidized gravity flows may include frequent small events as well as larger sedimentation events associated with major explosive eruptions.

Perhaps the most surprising finding in the bathymetry and sidescan imagery is the large number of submarine eruptive vents around Anatahan (Figs. 4–8). Eruptive vents were mapped at the summit of every *cone* and at the upslope end of every *lava flow* within the map area. Seventy-eight submarine eruptive vents are mapped and all lie within the volcanic edifices of Anatahan and NE Anatahan (within the outlines of the two volcaniclastic aprons), except one vent that is located in the middle of the abyssal channel SW of the island (Fig. 4). The closest vent to the island is only 1.3 km east of the shoreline at a depth of 350 m and the farthest is 19 km to the SW at 2950 m depth, but most are found between the depths of 300–2100 m and the radial distances of 5–17 km (Fig. 9). Of these submarine eruptive vents, 12 are associated with *lava flows* and 66 are atop *cones*. Some of the vents on the *cones* are aligned, probably indicating that they formed during radial dike intrusions that lead to fissure eruptions (Fig. 6). Sixty-two of the 78 eruptive vents (80%) are located in a dense concentration on the east side of the island (Figs. 4 and 9). Many of these east-side vents are located in the saddle between Anatahan and NE Anatahan, suggesting that this is a recent area of enhanced volcanism (Figs. 4 and 5). A similar pattern

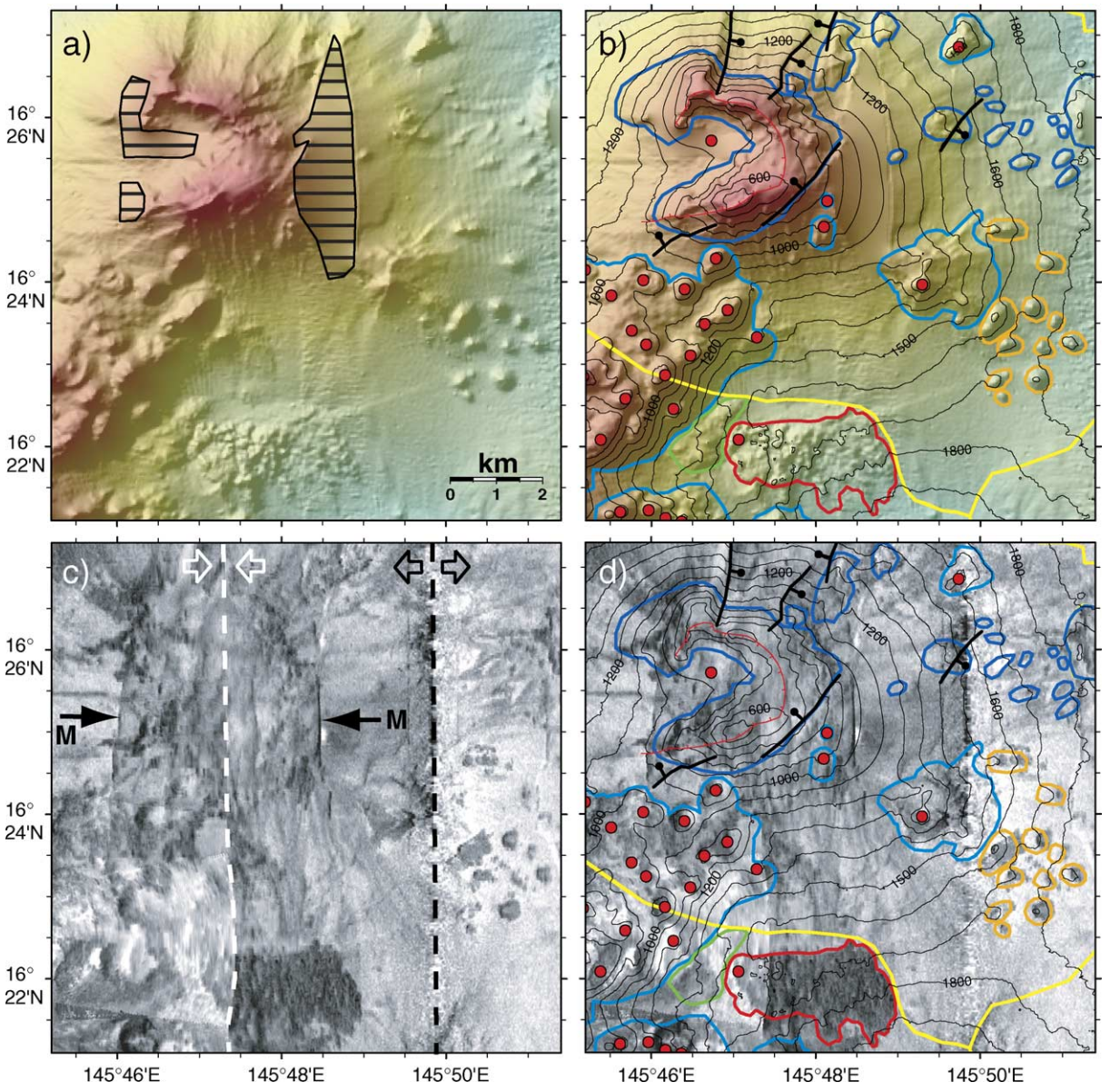

Fig. 5. Maps of area that includes the summit of NE Anatahan volcano with its large crater (upper left) and deposits interpreted to be landslide blocks on the SE flank (lower right). Location of map area is shown in Figs. 2 and 3. The cluster of cones in the saddle between Anatahan and NE Anatahan is in the lower left and a lava flow with rugged surface texture and high acoustic reflectivity is prominent at lower middle. (a and b) Shaded relief bathymetry as in Fig. 2. Outlined areas with horizontal lines in (a) are data gaps with interpolation. (c and d) Sidescan sonar imagery as in Fig. 3. Black dashed lines in (c) are towfish tracklines, white dashed lines are boundaries between adjacent swaths, and open arrows show insonification direction. Solid arrows labeled "M" in (c) show linear artifacts from acoustic multiples. Colored outlines and symbols in (b) and (d) correspond to geologic units and structures explained in Fig. 4. Contours in (b) and (d) are at an interval of 100 m. Note the angular shapes and high reflectivity contrast of the landslide blocks in (c).

Table 2
Areas and volumes of Anatahan and NE Anatahan volcanoes

Description	Area ($\times 10^6$ m^3)	Volume (km^3)
Anatahan island only	33	8.7
Anatahan volcano (including island)[a]	710	620
NE Anatahan volcano[b]	91	40
Anatahan and NE Anatahan combined	801	660

[a] Includes subaerial and submarine parts of Anatahan volcano within the mapped area of the volcaniclastic apron in Fig. 4 and above a base level of 2500 m.

[b] Includes the parts of NE Anatahan volcano within the mapped area of the volcaniclastic apron in Fig. 4 and above a base level of 1700 m.

of spatially concentrated eruptive vents in-between adjacent volcano summits has been mapped on the Galapagos island of Isabela, and was interpreted as due to the interaction of the radial volcano stress fields (Chadwick and Howard, 1991; Chadwick and Dieterich, 1995). Other clusters of cones are located on the SE flank of Anatahan and create hummocky constructional morphology and relatively high acoustic reflectivity (Fig. 6). Individual cones are 800–1600 m in width and 100–200 m high (measured on the upslope side). The similar backscatter values within each cluster suggests that the cones are similar in age and may have been emplaced as a group within a single eruptive episode (Figs. 5, 6 and 8). Lava flows emerge from the lower ends of some cones (Fig. 6). Other lava flows are relatively isolated and appear to emerge from one or two sources (Fig. 7). Anatahan has a relatively large number of lava flows on its submarine flanks compared to other Mariana volcanoes, based on the sidescan imagery we collected in 2003 (Embley et al., 2003, 2004, unpublished data). However, even though there appears to be evidence for relatively young submarine eruptions at Anatahan, there was no reported evidence for submarine volcanic activity during the 2003 eruption.

The morphology of the *cones* suggests that they are either formed by submarine pyroclastic/hydroclastic processes, or alternatively as thick mounds of pillow lava. Craters are not observed on the tops of the cones in the bathymetry or sidescan imagery (Figs. 5, 6 and 8), but many are distinctly conical in morphology. Historically documented eruptions on the Juan de Fuca and Gorda mid-ocean ridges have shown that basaltic lava erupted at low effusion rates can form hummocky pillow mounds up to 75 m thick (Chadwick and Embley, 1994; Chadwick et al., 1995, 1998). Presumably, pillow lavas of intermediate composition could form even thicker constructs, like the clusters of *cones* mapped at Anatahan. On the other hand, submarine pyroclastic eruptions have been documented from silicic volcanoes in water depths of at least 1000 m and from mafic volcanoes in depths exceeding 2000 m (Clague et al., 2000; Head and Wilson, 2003; White et al., 2003; Wright et al., 2003), so an explosive origin for the *cones* unit is also plausible. If the cones are indeed pyroclastic, their distribution at Anatahan shows that explosive activity can occur down to a depth of at least 2000 m. Most of the *cones* are found above 2000 m, whereas the *lava flows* are all below 1500 m (Fig. 9), possibly reflecting a change in the eruptive style from explosive to effusive with depth. Ultimately, near-bottom observations or direct sampling will be required to determine the origin of the *cones* unit.

Eruptive vents that are the sources of *lava flows* are located between 1500 and 3000 m (Fig. 9). Some of these lava flows reach as far as 15–20 km from the coastline of the island. The average length of the 11 mapped lava flows is 4.2 ± 1.8 km, and the average area of the flows is $5.8 \pm 3.5 \times 10^6$ m^2. They are tens of meters thick (based on depth profiles across them) on slopes generally $\leq 10^\circ$, suggesting that they are probably mafic to intermediate in composition. The lava flow on the NW flank of Anatahan was fluid enough that at a distance of 4 km from the vent a narrow finger of lava 250 m wide flowed down an abyssal channel towards the west for 1.7 km (Fig. 7). The slope of that channel is about 3°.

Eruptive vents have not been mapped on the *bedrock outcrops* that radiate outward (downslope) from the submarine flanks (especially on the west side of Anatahan). This is because these ridges are interpreted to be rocky outcrops of massive lava flows or possibly exposed dikes. They have been eroded, fragmented, or partially buried by volcaniclastic debris from above, and so their relation to their original source vents is no longer clear.

The flanks of Anatahan are draped by volcaniclastic material that extends out from the island a distance of 15–20 km to the south and west (Figs. 4 and 7). Where it abuts NE Anatahan volcano, however, the Anatahan apron only extends 5 km from the island. The diameter

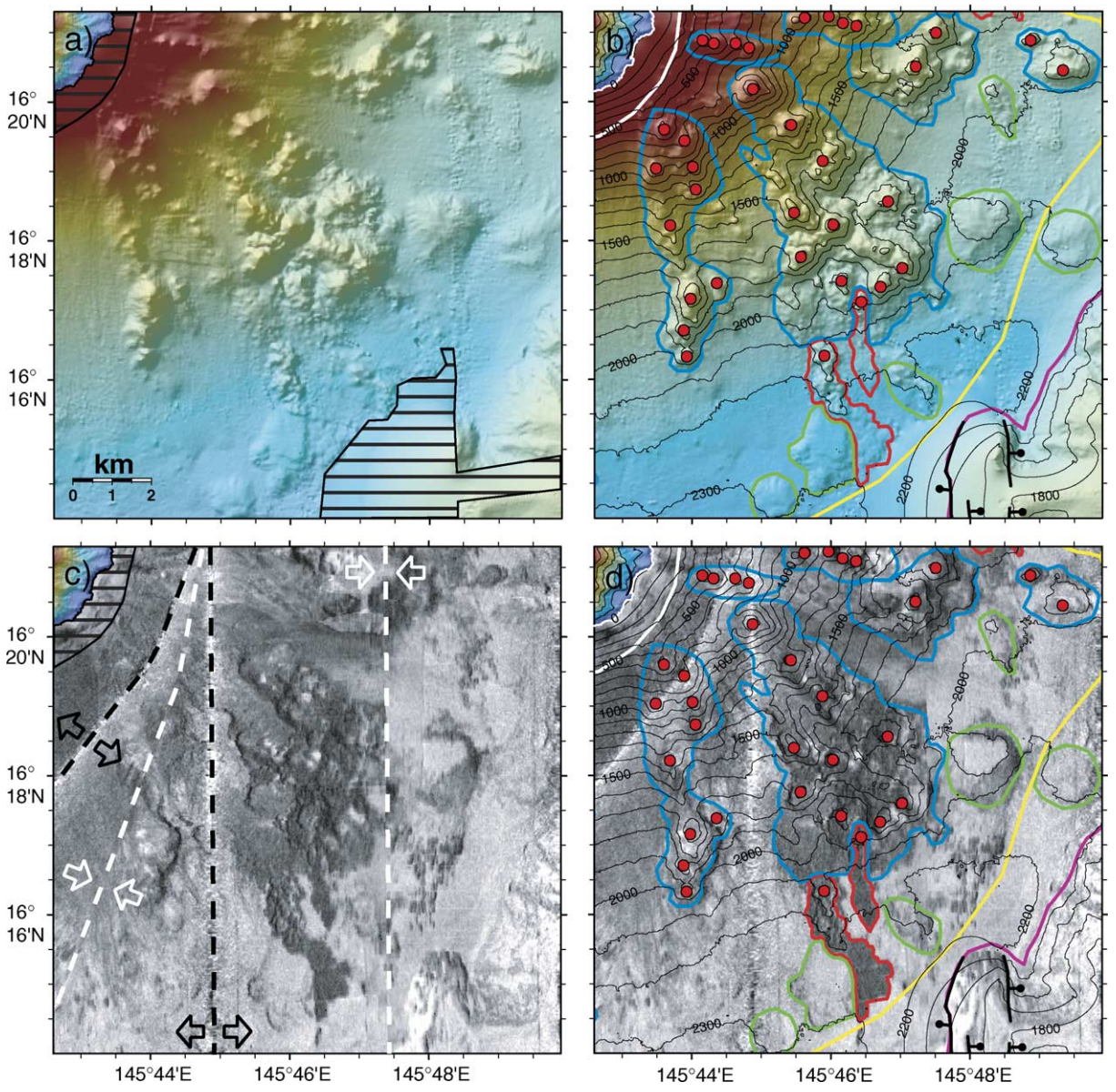

Fig. 6. Maps of area SE of Anatahan island (upper left) with large cluster of cones (center) and lava flows (lower middle). Location of map area is shown in Figs. 2 and 3. (a and b) Shaded relief bathymetry as in Fig. 2. Outlined areas with horizontal lines in (a) are data gaps with interpolation, and in (c) are areas of no valid sidescan data near the island. (c and d) Sidescan sonar imagery as in Fig. 3. Black dashed lines in (c) are towfish tracklines, white dashed lines are boundaries between adjacent swaths, and open arrows show insonification direction. Colored outlines and symbols in (b) and (d) correspond to geologic units and structures explained in Fig. 4. Contours in (b) and (d) are at an interval of 100 m. In (b) and (d) submarine eruptive vents (red dots) are mapped associated with cones and lava flows. Aligned eruptive vents (upper middle) suggest fissure eruptions along dikes.

of the *volcaniclastic apron* around Anatahan is about 3 times as large as the apron around NE Anatahan. The angles of the submarine slopes are generally 15–25° above 1000 m, 5–15° between 1000 and 2000 m, and <5° below 2000 m. In some cases, the material appears to be transported downslope as distinct flows that

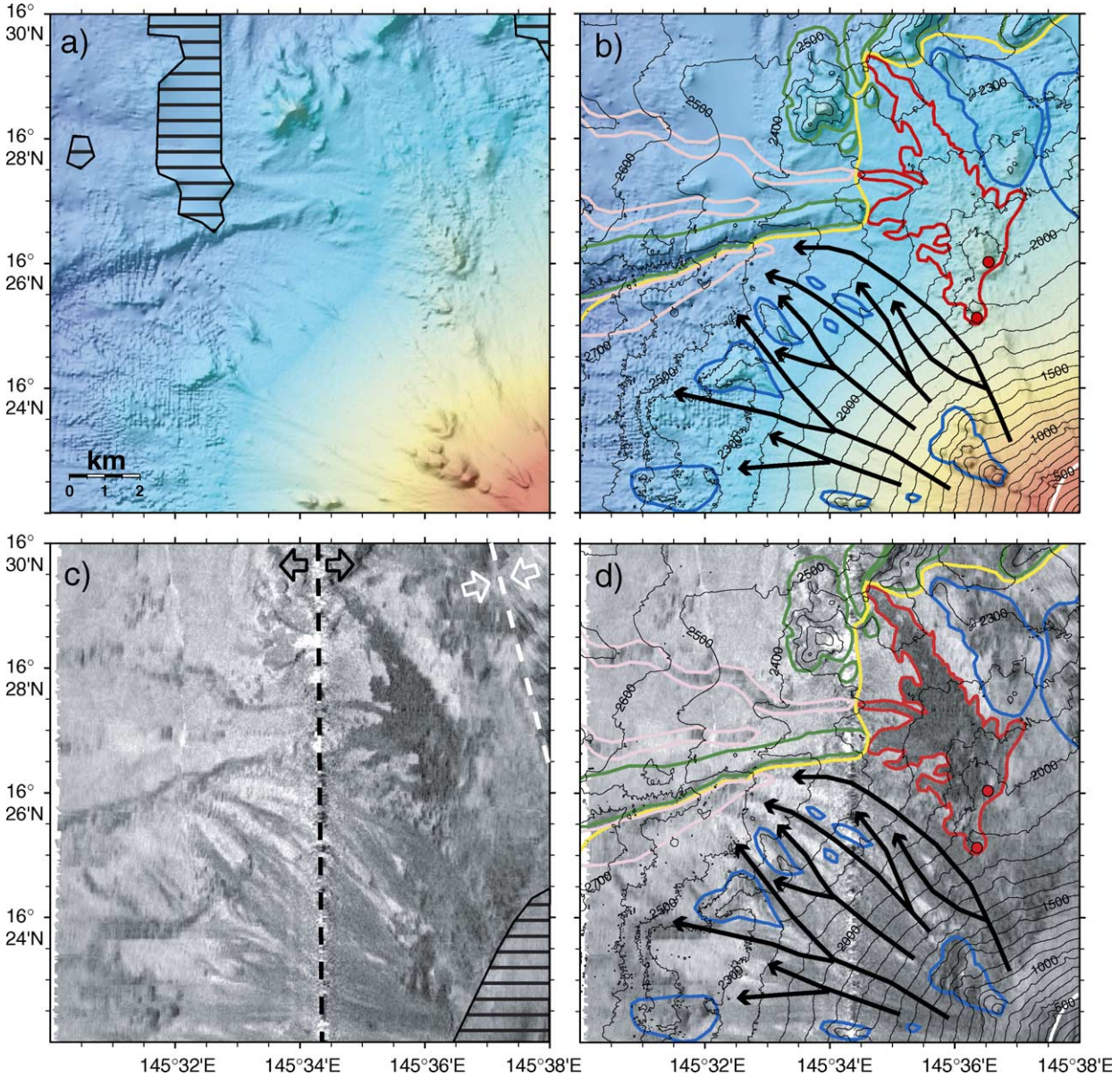

Fig. 7. Maps of area NW of Anatahan island showing braided channels of volcaniclastic debris shed from the upper slopes of the volcano. Location of map area is shown in Figs. 2 and 3. (a and b) Shaded relief bathymetry as in Fig. 2. Outlined areas with horizontal lines in (a) are data gaps with interpolation, and in (c) are areas of no valid sidescan data near the island. (c and d) Sidescan sonar imagery as in Fig. 3. Black dashed lines in (c) are towfish tracklines, white dashed lines are boundaries between adjacent swaths, and open arrows show insonification direction. Colored outlines and symbols in (b) and (d) correspond to geologic units and structures explained in Fig. 4. Contours in (b) and (d) are at an interval of 100 m. Flows of volcaniclastic debris are evident in the lower half of (c) as dark fingers of relatively higher acoustic reflectivity and are shown as curving black arrows in (b) and (d). The volcaniclastic flows are diverted by bedrock outcrops and constructional ridges, and ultimately flow into an abyssal channel (left middle).

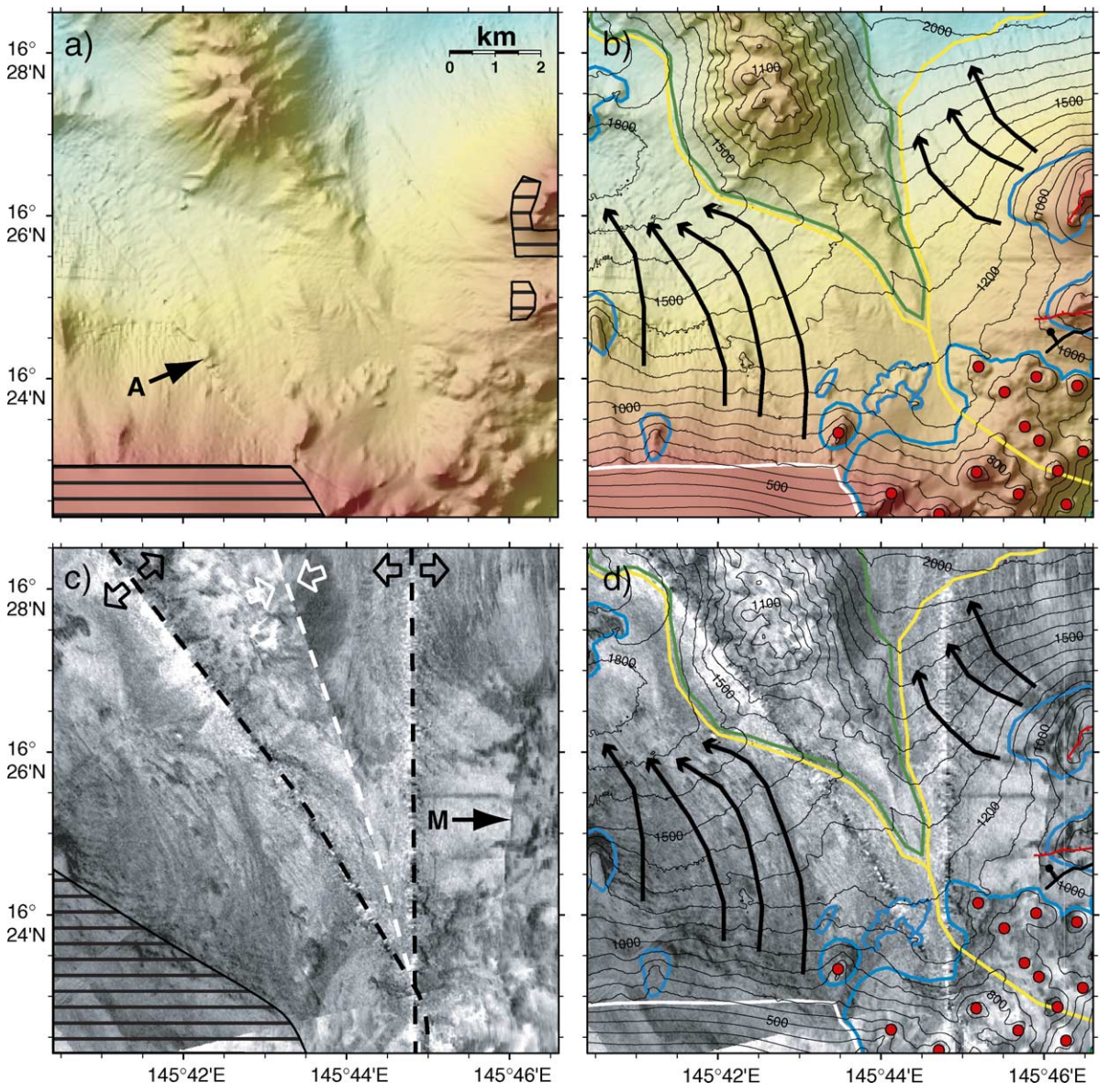

Fig. 8. Maps of area N of Anatahan island showing channels of volcaniclastic debris from Anatahan and NE Anatahan diverted around the large constructional ridge to the north of the island (upper middle). Also shown are submarine eruptive vents in the saddle between Anatahan and NE Anatahan volcanoes (lower right). Location of map area is shown in Figs. 2 and 3. (a and b) Shaded relief bathymetry as in Fig. 2. Outlined areas with horizontal lines in (a) are data gaps with interpolation, and in (c) are areas of no valid sidescan data near the island. Solid arrow labeled "A" in (a) points to linear artifact between EM300 and SeaBeam2000 data. (c and d) Sidescan sonar imagery as in Fig. 3. Black dashed lines in (c) are towfish tracklines, white dashed lines are boundaries between adjacent swaths, and open arrows show insonification direction. Solid arrow labeled "M" in (c) shows linear artifact from acoustic multiple. Colored outlines and symbols in (b) and (d) correspond to geologic units and structures explained in Fig. 4. Contours in (b) and (d) are at an interval of 100 m. Flows of volcaniclastic debris are evident in the lower left and upper right of (c) as dark fingers of relatively higher acoustic reflectivity and are shown as curving black arrows in (b) and (d). The deflection of the volcaniclastic flows from Anatahan and NE Anatahan indicates that the constructional ridge is older.

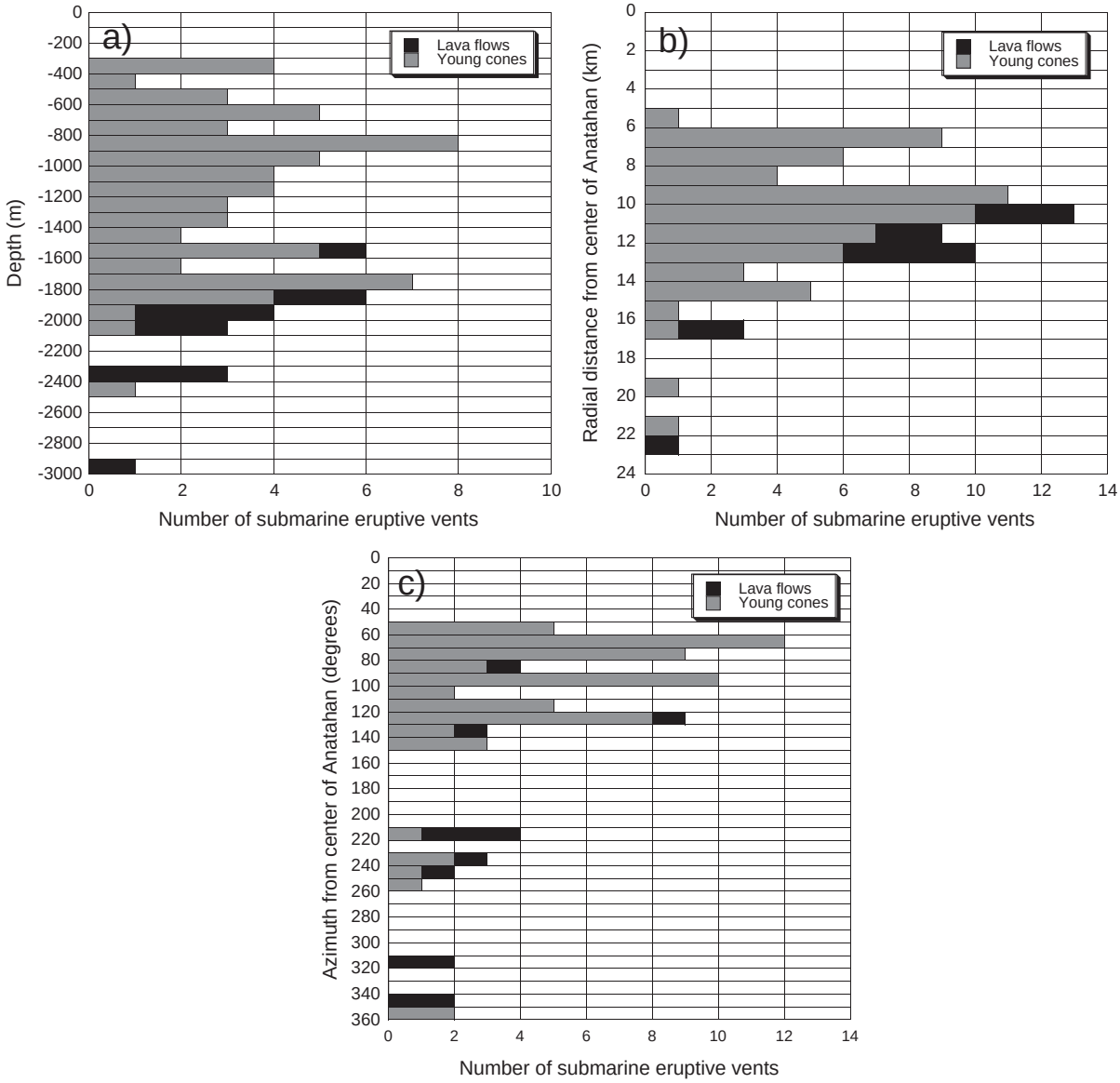

Fig. 9. Histograms showing the distribution of submarine eruptive vents at Anatahan volcano as a function of (a) depth, (b) radial distance from the center of Anatahan, and (c) azimuth from the center of Anatahan.

radiate outward in braided channels with slightly higher acoustic reflectivity than surrounding areas in the sidescan imagery (Fig. 7). For example, in the lower half of Fig. 7c relatively dark fingers (representing higher acoustic reflectivity) can be seen in the sidescan imagery on the NW submarine flank of Anatahan. The fingers extend from the upper edge of the sidescan coverage (~1000 m) down to depths below 2500 m. These appear to be channels that transport volcaniclastic debris downslope, because they occupy valleys, diverge around outcrops, and are diverted by a transverse *constructional ridge* at the bottom of the slope (Fig. 7). It is unclear why the channelized fragmental material has a higher acoustic reflectivity than its surroundings, but the channelized material may have a coarser grain size than the material

it is overriding. For example, the higher-reflectivity fingers could be younger in age and overly older deposits that are covered with fine-grained pelagic sediment (which would have lower reflectivity).

Similar flows of channelized volcaniclastic debris from Anatahan and NE Anatahan volcanoes (also appearing as relatively dark fingers in the sidescan imagery of Fig. 8) are deflected around a large *constructional ridge* located 5 miles north of the island. This linear ridge is 15 km long and 5 km wide, has a crest at a depth of 1000 m, and is aligned in the NNW–SSE direction. The deflection of the volcaniclastic debris around this linear ridge suggests that the ridge is older than both Anatahan and NE Anatahan volcanoes (Fig. 8).

The *older arc terrain* to the SE of Anatahan is heavily faulted (Fig. 4). All the faults appear to be normal faults with N–S strikes and pronounced vertical offsets, apparently reflecting tectonic extension in the E–W direction. Most of the faults in the *older arc terrain* face to the west toward the Mariana Trough, which is the current locus of backarc spreading (Karig et al., 1978; Martinez et al., 1995).

5. Conclusions

The submarine flanks of Anatahan volcano were surveyed in 2003 and 2004 with multibeam and sidescan sonars. These data provide new information on this active volcano, only the tip of which is exposed above sealevel (Fig. 10). For example, the area above sealevel is only 5% of the area of Anatahan's volcaniclastic apron (Table 2). Likewise, the volume of the island of Anatahan is 8.7 km^3, and is only 1% of the total volume of the volcano, which amounts to 620 km^3 (Table 2). NE Anatahan volcano adds an additional 40 km^3 to this volume (Table 2).

Geologic mapping of the submarine flanks of Anatahan reveals that there are many more eruptive vents below sealevel than above. We mapped 78 submarine eruptive vents, 12 of which are associated with *lava flows* and the remaining 66 are associated with *cones*. Most of the submarine eruptive vents are located on the east flank of the volcano. If the distribution of the *cones* indicates the depth range of submarine pyroclastic activity, then the transition from explosive to effusive eruptions takes place at a depth between 1500 and 2000 m.

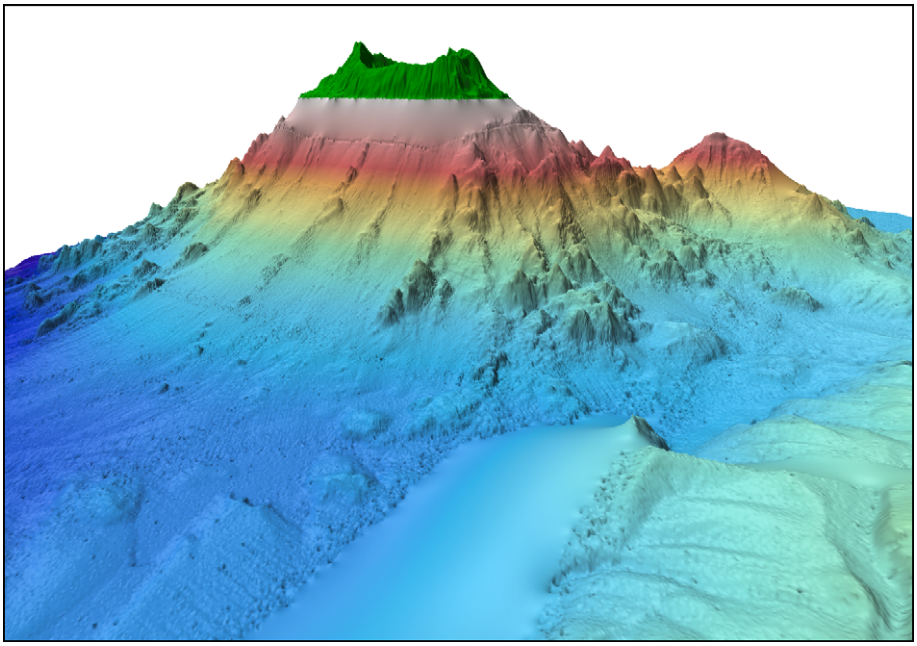

Fig. 10. Three-dimensional view of the combined bathymetry and topography of Anatahan volcano from the southeast, showing that the island (green) is only a small percentage of a much larger volcanic edifice. Vertical exaggeration is 3 times.

There are no major landslide deposits on the submarine slopes of Anatahan. This appears to be true of most of the other submarine volcanoes in the Mariana arc as well. This may be due to the felsic composition of the volcano, the predominance of unconsolidated volcaniclastic eruptive products, and the lack of well-defined rift zones. Arc volcanoes apparently do not grow outward and shed debris over the surrounding seafloor in the same way that oceanic basaltic volcanoes do.

Clearly, most of the eruptive products from Anatahan volcano are located below sealevel, but because none of these have been sampled the current view of the eruptive history of the volcano must be considered incomplete. It is hoped that this mapping effort will motivate a concerted submarine sampling program (using targeted dredges, rock cores, and/or submersible dives) in order to identify the compositions and ages of the various geologic units that we have mapped. This would shed additional light on the past activity of Anatahan, one of the largest active volcanoes in the Mariana arc.

Acknowledgements

Steve Schilling kindly provided the digital elevation model of Anatahan, and Frank Trusdell helped to georeference it with hand-held GPS positions. Scott Rowland provided other helpful digital data and discussion. The skills and support of the captain and crew of the *R/V Thomas G. Thompson* were critical to the success of our 2003 and 2004 Marianas cruises. In particular, Mike Realander, Bill Martin, and Rob Hagg provided valuable assistance at sea in collecting the EM300 data. The Hawaii Undersea Mapping Group at University of Hawaii did an excellent job operating the MR1 sidescan sonar during our 2003 survey. Mr. Gun Tae Park collected the Seabeam 2000 data on the *R/V Onnuri* in September 2003, with the assistance of Mr. Minkyu Park and Dr. Robert Dziak, who acted as co-chief scientists on that cruise. The manuscript was improved by helpful reviews by Scott Rowland and Dave Clague. This research was supported by the NOAA Ocean Exploration and Vents Programs. This is PMEL contribution number 2728.

References

Bloomer, S.H., Stern, R.J., Smoot, N.C., 1989. Physical volcanology of the submarine Mariana and volcano arcs. Bulletin of Volcanology 51, 210–224.

Borgia, A., 1994. Dynamic basis of volcanic spreading. Journal of Geophysical Research 99 (B9), 17791–17804.

Borgia, A., Ferrari, L., Pasquare, G., 1992. Importance of gravitational spreading in the tectonic and volcanic evolution of Mount Etna. Nature 357, 231–235.

Caress, D.W., Spitzak, S.E., Chayes, D.N., 1996. Software for multibeam sonars. Sea Technology 37, 54–57.

Chadwick Jr., W.W., Dieterich, J.H., 1995. Mechanical modeling of circumferential and radial diking on Galapagos volcanoes. Journal of Volcanology and Geothermal Research 66 (1–4), 37–52.

Chadwick Jr., W.W., Embley, R.W., 1994. Lava flows from a mid-1980s submarine eruption on the Cleft Segment, Juan de Fuca Ridge. Journal of Geophysical Research 99 (B3), 4761–4776.

Chadwick Jr., W.W., Howard, K.A., 1991. The pattern of circumferential and radial eruptive fissures on the volcanoes of Fernandina and Isabela Islands, Galapagos. Bulletin Volcanologique 53, 259–275.

Chadwick Jr., W.W., Embley, R.W., Fox, C.G., 1995. SeaBeam depth changes associated with recent lava flows, CoAxial segment, Juan de Fuca Ridge: evidence for multiple eruptions between 1981–1993. Geophysical Research Letters 22 (2), 167–170.

Chadwick Jr., W.W., Embley, R.W., Shank, T.M., 1998. The 1996 Gorda ridge eruption: geologic mapping, sidescan sonar, and SeaBeam comparison results. Deep-Sea Research II 45 (12), 2547–2570.

Clague, D.A., Davis, A.S., Bishchoff, J.L., Dixon, J.E., Geyer, R., 2000. Lava bubble-wall fragments formed by submarine hydrovolcanic explosions on Loihi Seamount and Kilauea Volcano. Bulletin of Volcanology 61, 437–449.

Dieterich, J.H., 1988. Growth and persistence of Hawaiian volcanic rift zones. Journal of Geophysical Research 93 (B5), 4258–4270.

Embley, R.W., et al., 2003. New mapping of Mariana submarine volcanoes with sidescan and multibeam sonars. Eos Transactions American Geophysical Union 84, T32A-0913 ((46, Fall Meet. Suppl.): Abstract).

Embley, R.W. et al. 2004. Explorations of Mariana arc volcanoes reveal new hydrothermal systems. Eos Transactions American Geophysical Union, 85 (4): 37, 40.

Head, J.W., Wilson, L., 2003. Deep submarine pyroclastic eruptions: theory and predicted landforms and deposits. Journal of Volcanology and Geothermal Research 121, 155–193.

Holcomb, R.T., Searle, R.C., 1991. Large landslides from oceanic volcanoes. Marine Geotechnology 10, 19–32.

Karig, D.E., Anderson, R.N., Bibee, L.D., 1978. Characteristics of back arc spreading in the Mariana Trough. Journal of Geophysical Research 83 (B3), 1213–1226.

Lénat, J.F., Vincent, P., Bachèlery, P., 1989. The off-shore continuation of an active basaltic volcano: Piton de la Fournaise (Reunion Island, Indian Ocean); structural and geomorpholog-

ical interpretation from Sea Beam mapping. Journal of Volcanology and Geothermal Research 36, 1–36.

Martinez, F., Fryer, P., Baker, N.A., Yamazaki, T., 1995. Evolution of backarc rifting; Mariana Trough, 20 degrees −24 degrees N. Journal of Geophysical Research 100 (B3), 3807–3827.

Moore, J.G., Chadwick Jr., W.W., 1995. Offshore geology of Mauna Loa and adjacent areas, Hawaii. In: Rhodes, J.M., Lockwood, J.P. (Eds.), Mauna Loa Revealed: Structure, Composition, History and Hazards. J. Geophys. Monograph, vol. 92. American Geophysical Union, Washington, DC, pp. 21–44.

Moore, J.G., et al., 1989. Prodigious submarine landslides on the Hawaiian ridge. Journal of Geophysical Research 94, 17465–17484.

Nakamura, K., 1980. Why do long rift zones develop in Hawaiian volcanoes—a possible role of thick oceanic sediments (in Japanese). Bulletin of the Volcanological Society of Japan 25, 255–267.

Rowland, S.K., Lockwood, J.P., Trusdell, F.A., Moore, R.B., Sako, M.K., Koyanagi, R.Y., Kojima, G., 2005. Anatahan, Northern Mariana Islands: reconnaissance geological observations during and after the volcanic crisis of spring 1990, and monitoring prior to the May 2003 eruption. Journal of Volcanology and Geothermal Research 146, 26–59 (this issue).

Stern, R.J., Hargrove, U.S., 2003. The Anatahan Felsic Province in the Mariana Arc system. Eos Transactions American Geophysical Union 84, V32B-1010 ((46 Fall Meet. Suppl.): Abstract).

Stern, R.J., Fouch, M.J., Klemperer, S.L., 2003. An overview of the Izu-Bonin-Mariana subduction factory. In: Eiler, J. (Ed.), Inside the Subduction Factory. Geophys. Monograph, vol. 138. American Geophysical Union, Washington, DC, pp. 175–222.

Tanakadate, H., 1940. Volcanoes in the Marian Islands in the Japanese Mandated South Seas. Bulletin of Volcanology 6, 199–225.

Trusdell, F.A., Moore, R.B., Sako, M., White, R.A., Koyanagi, S.K., Chong, R., Camacho, J.T., 2005. The 2003 eruption of Anatahan Volcano, Commonwealth of the Northern Mariana Islands: chronology, volcanology, and deformation. Journal of Volcanology and Geothermal Research 146, 184–207 (this issue).

Wessel, P., Smith, W.H.F., 1991. Free software helps map and display data. Eos Transactions American Geophysical Union 72, 441.

White, J.D.L., Smellie, J.L., Clague, D.A., 2003. Introduction: a deductive outline and topical overview of subaqueous explosive volcanism. In: White, J.D.L., Smellie, J.L., Clague, D.A. (Eds.), Explosive Subaqueous Volcanism. Geophysical Monograph, vol. 140. American Geophysical Union, Washington, DC, pp. 1–23.

Wiens, D.A., et al., 2004. Observing the historic eruption of Northern Mariana Islands volcano. Eos Transactions American Geophysical Union 85 (1): 2, 4.

Wright, I.C., Gamble, J.A., Shane, P.A.R., 2003. Submarine silicic volcanism of the Healy caldera, southern Kermadec arc (SW Pacific): I. Volcanology and eruption mechanisms. Journal of Volcanology and Geothermal Research 65, 15–29.